Environmental Research 199 (2021) 111252

Contents lists available at ScienceDirect

Environmental Research

journal homepage: www.elsevier.com/locate/envres

Characterization of the synergistic relationships between nitrification and microbial regrowth in the chloraminated drinking water supply system

Xiaocao Miao, Xiaohui Bai *

State Key Laboratory of Microbial Metabolism, Joint International Research Laboratory of Metabolic & Developmental Sciences, School of Life Sciences and Biotechnology, Shanghai Jiao Tong University, Shanghai, 200240, PR China

ARTICLE INFO

Keywords:
Drinking water
Chloramine disinfection
Microbial regrowth
Incomplete nitrification
Metabolic mechanism

ABSTRACT

Deterioration of water quality is commonly found in secondary water supply systems (SWSSs), especially the growth of microbes. To explore the metabolic mechanism for rapid microbial regrowth in SWSSs, a regrowth potential assessment, flow cytometry, and quantitative PCR were conducted. Metagenomic and 16S rRNA gene sequencing were performed to better understand the microbial communities and metabolism. It was found that the increased biomass in the SWSS was significantly higher than that in the drinking water distribution system (DWDS). Statistical analysis revealed that ammonia oxidation was the dominant driver of increased biomass in the SWSS. The abundances of ammonia oxidation bacteria, concentration of nitrogen species, and related enzymes demonstrated that ammonia oxidation in the SWSS was more vigorous than that in the DWDS. In the SWSS, the metabolism of the ammonia oxidation cluster was more vigorous, and ammonia-oxidizing bacteria (AOB) were the dominant nitrifying bacteria. Incomplete nitrification products were involved in the metabolism of heterotrophic bacteria and promoted the growth of heterotrophic bacteria in the SWSS. More attention should be given to controlling incomplete nitrification to improve tap water quality.

1. Introduction

Deterioration of water quality is commonly found in communities in metropolitan cities and in particular, it consists of bacterial and fungal growth (Li et al., 2018; Liu et al., 2017). Despite constant improvements to the water purification process, contaminants (e.g., chlorine-tolerant bacteria and organic and odor compounds) could not be removed completely from the influent and can always be found in SWSSs (Matsui et al., 2015; Zamyadi et al., 2015; Liu et al., 2017; Nescerecka et al., 2018).

Traditional purification processes are inefficient in removing all contaminants in drinking water treatment systems (DWTSs), there is still some contaminants left in the effluent (Prest et al., 2016). Long stagnation in DWDSs and exogenous microbial invasions from building infrastructures in SWSSs can promote microbial growth (Li et al., 2018; Liu et al., 2018). Long water retention times and low disinfectant concentrations together affect microbial community structures and compositions (Douterelo et al., 2013; Li et al., 2018; Xu et al., 2018). Therefore, water in SWSSs usually contains a physical load (particles), nutrient load (organic and inorganic nutrients), and biological load (cells) (Liu et al., 2017). The causes of deteriorating tap water quality have previously been explored, as mentioned above. However, it is not clear which factor has greater consequences.

As one of the factors that affects water quality, nitrification is an increasing concern worldwide (Zhang et al., 2009; Tatari et al., 2017; Wang et al., 2017; Albers et al., 2018). Nitrification, which consists of ammonia oxidation and nitrite oxidation, is widely observed in drinking water supply systems (Wagner et al., 2018). Nitrifiers have also been found in the biofilms of tropical drinking water (Cruz et al., 2020). In chloraminated DWTSs, chloramine use can promote the growth of nitrifying bacteria and nitrification (Regan et al., 2003). Nitrification contributes to monochloramine depletion and results in nitrate formation, which can lead to unsafe water and water eutrophication (Berry et al., 2006). Several studies have reported a positive correlation between nitration products and the number of bacteria (Regan et al., 2003; Zhang et al., 2009). However, the relationships between nitrification and microbial regrowth and how nitrification affects biomass in chloraminated drinking water supply systems remain largely unknown.

This research focused on the metabolic mechanism of greater microbial regrowth in SWSSs. This was achieved by revealing the interactions among bacteria, fungi, and algae in water supply systems. We focused on studying the synergistic relationships between nitrification

* Corresponding author.
E-mail address: xhbai@sjtu.edu.cn (X. Bai).

https://doi.org/10.1016/j.envres.2021.111252
Received 1 January 2021; Received in revised form 23 April 2021; Accepted 26 April 2021
Available online 18 May 2021

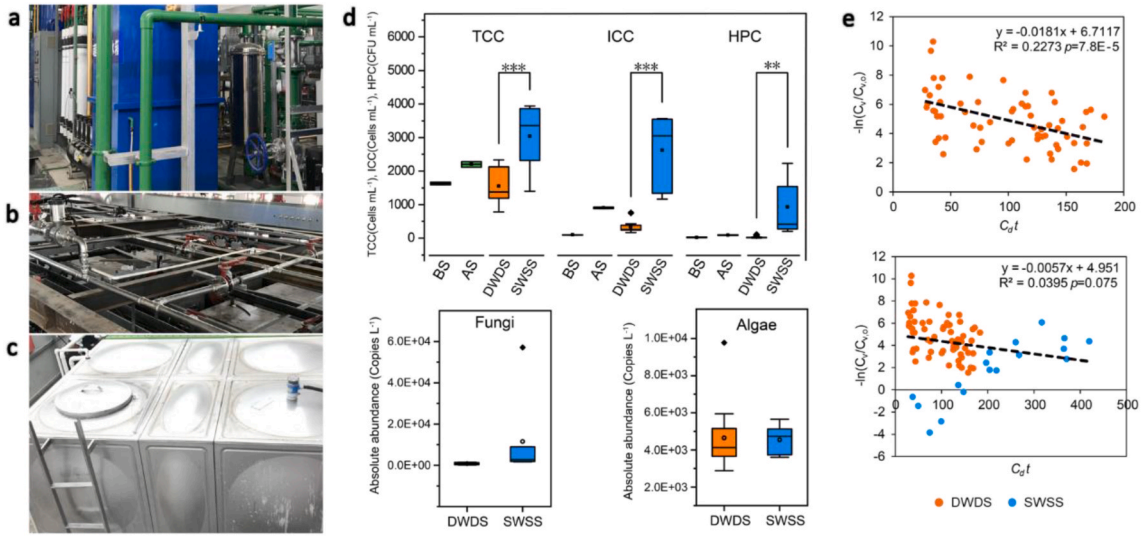

Fig. 1. The experimental facility of a pilot-scale drinking water supply system included DWTS (a), DWDS (b), and SWSS (c). Comparison of the changes in biomass, including ICC, HPC, fungi, and algae, in real samples (DWDS and SWSS) and effluent (kept stagnation for 8 days) by using Fisher's LSD test (d). BS: before stagnation, AS: after stagnation, and ***: $p < 0.001$; **: $p < 0.01$. Comparison of bacterial inactivation of the water in and out of the SWSS by the chloramine disinfectant (e).

and microbial regrowth.

2. Materials and methods

2.1. Sample collection

The research was conducted in a full-scale drinking water treatment plant and the corresponding distribution network in Shanghai, China. This plant treats surface water from the Jinze reservoir that is originally supplied from Taihu Lake, and its production rate was 3×10^5 m^3 d^{-1}. Water samples were collected from a full-scale DWTS (raw water, after sedimentation, after sand filtration, after ozonation, after biological activated carbon (BAC), and after chloramine disinfection), the corresponding distribution system which consisted of ductile iron pipes with diameters ranging from 300 to 1600 mm, and the corresponding SWSS in communities (Fig. S1). A stainless steel water tank was selected for pilot-scale experimental research because it is widely used in SWSSs. Water samples were taken after 5 min of flushing and were collected by using disinfected 10 L bottles at each location. All samples were transported on ice to the laboratory and were processed within 12 h.

2.2. Analysis of water quality and disinfection kinetics

The total residual chlorine and temperature parameters were measured in situ. Total dissolved solids (TDS), total organic carbon (TOC), pH, dissolved oxygen, alkalinity, nitrite, nitrate, heterotrophic plate counts (HPC), and assimilable organic carbon (AOC) were measured in the laboratory (Zhang T, 2007; Lautenschlager et al., 2013). Enumeration of total cell concentrations (TCC) and intact cell concentrations (ICC) by flow cytometric measurements (FCM) was performed by using SYTO 9 stain and propidium iodide (Lehtinen et al., 2004). FCM measurements were performed with a CytoFLEX flow cytometer (Beckman Coulter, Inc.USA).

A total of 81 water samples for inactivation kinetics analysis were taken from May 2018 to August 2019. The chloramine inactivation mechanics were evaluated by observing the functional relationship between microbial inactivation (reduction of HPC) and test times (water stagnation times). The inactivation kinetics were fitted to a first-order Chick-Watson model:

$$\ln \frac{C_v}{C_{v,0}} = k_{CW} C_d t$$

where k_{CW} is the inactivation rate constant, C_d is the disinfectant concentration, and C_v is the concentration of infective bacteria (Sigstam et al., 2013).

2.3. Assessment of regrowth potential

The microbial regrowth potential was assessed by using a pilot-scale experimental facility, which consisted of a DWTS, DWDS, and SWSS (Fig. 1a, b, c). The water purification process, pipe material (ductile iron), and water tank (stainless steel) were the same as those of the actual system. The total volume of the tank was 7.5 m^3. The inner wall of the tank was completely cleaned before the experiments commenced. After chloraminated water entered the tank, the water was allowed to stagnate for eight days, and water quality measurements were performed every two days.

2.4. DNA extraction and quantification

Biomass from the water was collected by the membrane filtration method. Two liters of water were filtered through a sterile 0.22 μm mixed cellulose membrane (Bandao, China) by using a magnetic filter funnel (Pall Life Science, USA) and vacuum pressure pump (Pall Life Science, USA). Genomic DNA was extracted from the membrane by using an optimized phenol:chloroform-based method (Douterelo et al., 2013). In brief, each filter was cut into small pieces and placed in 2 mL tubes. The following lysis buffer, 800 μL of 2 × CTAB lysis buffer (2% CTAB (w/v), 0.1 M Tris-HCl, 0.05 M EDTA, pH=8.0, 1.4 M NaCl, pH 8), 2 μL of beta-mercaptoethanol, and 0.3 g of glass beads, was added to the tube and then mixed with an oscillator for 10 min. The tubes were lapped for 3 min (30 Hz). Twenty microliters of protease K (20 mg mL^{-1}) were added, and the tubes were incubated at 65 °C for 1 h. The supernatant was extracted twice with 800 μL of phenol:chloroform:isoamyl alcohol (25:24:1), pH 8, and 800 μL of chloroform:isoamyl alcohol (24:1). DNA was precipitated with a 0.6 volume of isopropyl alcohol and 0.1 volume of NaAc (3 M) overnight and then washed in 500 μL of 70% ethanol three times. 40 μL of sterile water was added to the dry tube. The DNA concentration was detected by a OneDrop OD-1000 spectrophotometer. DNA quality was checked by 2% agarose gel electrophoresis. Moreover, the qualified DNA was adjusted to a concentration of 50 ng μL^{-1} and stored at −80 °C.

2.5. Quantitative PCR

Quantification of the sum of Nitrosomonas plus Nitrospira, Nitrospira, fungi, and algae was performed by 16S rRNA gene-targeted quantitative PCR (qPCR) with a Bio-Rad CFX Manager system. The qPCR primers used are described in the supplementary information (Tab. S2). The DNA template (1 μL) and appropriate primers (1 μL) were combined with HieffTM qPCR SYBR® Green Master Mix (YEASEN) to create 20 μL reaction volumes. The thermal cycling conditions were the same as those published in previous studies (Graham et al., 2007; Gülay et al., 2016). The absolute abundance of each gene was calculated by the formula mentioned earlier (Looft et al., 2012; Zheng et al., 2018; Chen et al., 2019). For all samples, amplification was confirmed with more than two positive replicates.

2.6. Illumina sequencing of 16S, ITS, and 23S rRNA genes

All samples for Illumina sequencing were taken in May 2018. The V3–V4 hypervariable regions of the bacterial 16S rRNA gene were amplified with the 338F and 806R primers (Mori et al., 2014). The internal transcribed spacer (ITS) regions of fungi were amplified with the primers ITS1F and ITS2R (Adams et al., 2013). Furthermore, domain V of the 23S plastid rRNA gene in the eukaryotic algal and cyanobacterial groups was amplified with primers p23SrV_f1 and p23SrV_r1 (Sherwood and Presting, 2007; Pfendler et al., 2018). The purified amplicons were sequenced on an Illumina MiSeq platform (Illumina, San Diego, USA) (Xie et al., 2016).

Raw fastq files were demultiplexed, quality-filtered by Trimmomatic and merged by FLASH (Bolger et al., 2014). Operational taxonomic units (OTUs) were clustered with a 97% similarity cutoff for the 16S-, ITS- and 23S-generated sequences using UPARSE; furthermore, chimeric sequences were identified and removed by using UCHIME (Edgar et al., 2011; Edgar, 2013). The taxonomy was analyzed by QIIME and by the Ribosomal Database Project (RDP) Classifier algorithm with a confidence threshold of 70% (Wang et al., 2007). The 16S, ITS, and 23S taxonomic assignments were performed using Silva Seed v128, UNITE v7.0, and the NCBI database, respectively (Quast et al., 2012; Pfendler et al., 2018; Nilsson et al., 2019).

2.7. Shotgun metagenomic sequencing and quality control

Six representative samples were selected for shotgun metagenomic sequencing, which included those from raw water, effluent water, two samples from the DWDS (with minimum and maximum pipe lengths), roof tank water, and ground tank water. Sequencing was performed by using Illumina Hiseq 2000. Libraries were prepared with a fragment length of approximately 400 bp by using Covaris M220 and NEXTFLEX™ Rapid DNA-Seq Kit. Raw reads were quality controlled using fastq (Chen et al., 2018). A total of 256,210,800 clean reads were generated across all six samples with an average of 42,701,800 reads per sample. CD-HIT (http://www.bioinformatics.org/cd-hit/), SOAPaligner, and BLASTP were used for abundance calculations of nonredundant gene sets, as well as annotation of KEGG orthologies and modules (Zhang et al., 2019; Li et al., 2009).

2.8. Statistical analysis

All data used in this study were considered to be statistically significant at $p < 0.05$ unless indicated otherwise. All environmental variables were evaluated using one-way univariate analysis of variance (ANOVA) to select reasonable measurements. Mothur 1.30.1 was used to estimate alpha diversity, including the Shannon diversity index, ACE index, and Chao index (Schloss et al., 2009). Comparisons of microbial community structures were displayed by using two axes of a nonmetric multidimensional scaling (NMDS) analysis based on Bray-Curtis distances at the genus taxonomic level, and analysis of similarity (ANOSIM) was conducted to determine whether the community differences were significant. Fisher's least significant difference (LSD) test was used to analyze the dissimilarities of environmental variables in different groups. Linear discriminant analysis (LDA), coupled with effect size measurement analysis (LEfSe), was performed to search for the biomarkers of different groups (Segata et al., 2011). Additionally, the Wilcoxon rank-sum test was conducted to identify differentially abundant features (Dixon, 2003). Co-occurrence networks of microorganism approaches were created by the "WGCNA" package and Gephi (Bastian and H.S, 2009). The functional groups of the bacterial and fungal OTUs were inferred using FARPROTAX and FUNGuild v1.1 (Louca et al., 2016; Nguyen et al., 2016). The main microbial predictors for biomass were

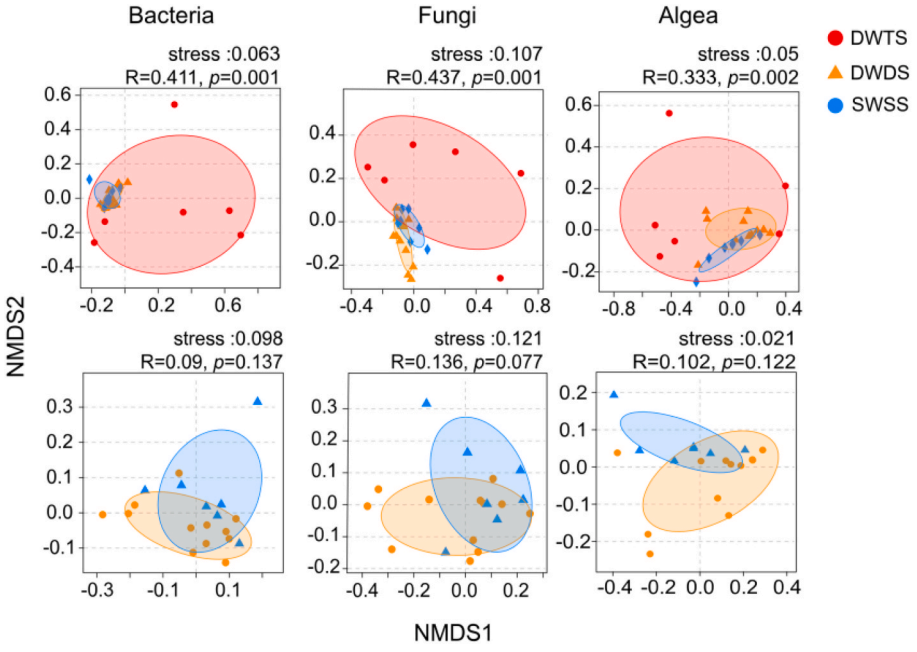

Fig. 2. Dissimilarities in the community compositions of bacteria, fungi, and algae among different water subsystems. The nonmetric multidimensional scaling analysis was based on Bray-Curtis distances.

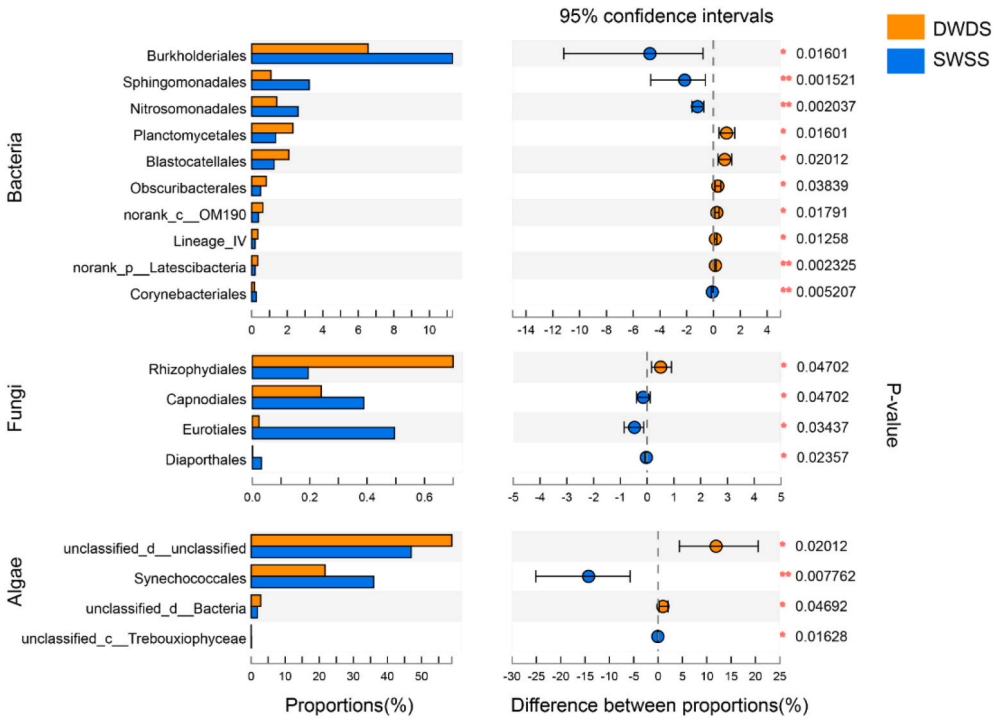

Fig. 3. Wilcoxon rank-sum test of bacteria, fungi, and algae at the order level between DWDS and SWSS.

identified by a classification random forest (RF) analysis by using the "A3", "rfPermute", and "relaimpo" packages (Jiao et al., 2018).

3. Results

3.1. Large biomass increase in SWSS and regrowth potential assessment

Twenty-five samples from a full-scale drinking water supply system were analyzed. The average TOCs from the DWDS to SWSS were 3.06 and 3.03 mg L^{-1}, respectively. The average TDSs from the DWDS to SWSS were 369.65 and 371.89 mg L^{-1}, respectively (Fig. S2). There were no significant differences between the DWDS and SWSS for either the TOCs or TDSs. Therefore, the physiochemical water quality was stable in the pipe system.

The ICCs decreased during the full-scale water purification process and stabilized at a low level in the DWDS but increased sharply after flowing into the SWSS (Fig. S3). The biomass indexes of ICC and HPC in the DWDS and SWSS were found to be significantly different ($p < 0.01$) (Fig. 1d). The absolute fungal abundances were also higher in the SWSS than in the DWDS, but no significant differences were found. There were no significant differences in the absolute abundances of algae between the two subsystems.

To explore the effect of chloramine decay as a single factor on biomass growth, a pilot-scale water tank experiment was conducted, and the freshwater biomass was compared to that of stagnant water (Fig. 1d, Fig. S4). It was found that the amount of biomass increased slightly after eight days of stagnation. Bacterial regrowth in the tank ranged from 2- to 5-fold after a few days of stagnation. In contrast, the bacterial regrowth of real household tap water in the SWSS ranged from 7- to 78-fold, which far exceeded the full-scale tank experiment. Furthermore, there were no significant differences ($p > 0.05$) between the biomass of water before stagnation (BS) and after stagnation (AS). Therefore, apart from the retention time and chloramine decay, there must be other causes for the great increase in biomass in SWSS.

The inactivation kinetics for bacteria in the DWDS and SWSS are shown in Fig. 1e. The inactivation rate constant in the DWDS was 0.0181, but the Chick-Watson model of chloramine disinfection kinetics failed to build ($p > 0.05$) when the SWSS was considered. The differences in the chloramine disinfection kinetic models between the DWDS and SWSS suggested that the responses of microorganisms to chlorine were different.

3.2. Microbial community compositions

The rarefaction curves reached a plateau, which suggested that the sequencing data can reflect the vast majority of biodiversity information in the samples (Fig. S5). Good's coverage ranged between 0.983 and 0.999 for all samples, which suggested that the results of this sequencing can reflect the real situation of microbes in the samples (Fig. S6). The sequencing and diversity information are described in the supplementary information (Tab. S3-6).

NMDS analysis revealed that the water samples from different subsystems formed clusters in the ordination space (Fig. 2). ANOSIM revealed significant differences ($p < 0.05$) in microbial community structures among the DWTS, DWDS, and SWSS (p=0.001, p=0.001, and p=0.002, respectively). However, no significant differences ($p > 0.05$) between the DWDS and SWSS community compositions were observed. As a result, the biological communities in the DWDS and SWSS was similar, and exogenous microbial invasion from secondary water supply facilities was limited.

LDA coupled with LEfSe analysis was conducted to compare the biological compositions of bacteria, fungi, and algae, which showed significant results (LDA score [log10]> 3.5) among different subsystems (Fig. S7). Considering the lack of significant differences ($p > 0.05$) in community compositions between the DWDS and SWSS by NMDS analysis, the Wilcoxon rank-sum test between the DWDS and SWSS was analyzed (Fig. 3). The microbes with increased abundance ($p < 0.01$) in the SWSS included Burkholderiales, Sphingomonadales, Nitrosomonadales, Capnodiales, Eurotiales, Diaporthales, Synechococcales, and Trebouxiophyceae.

3.3. Microbial function prediction

The results of bacterial and fungal function predictions showed that

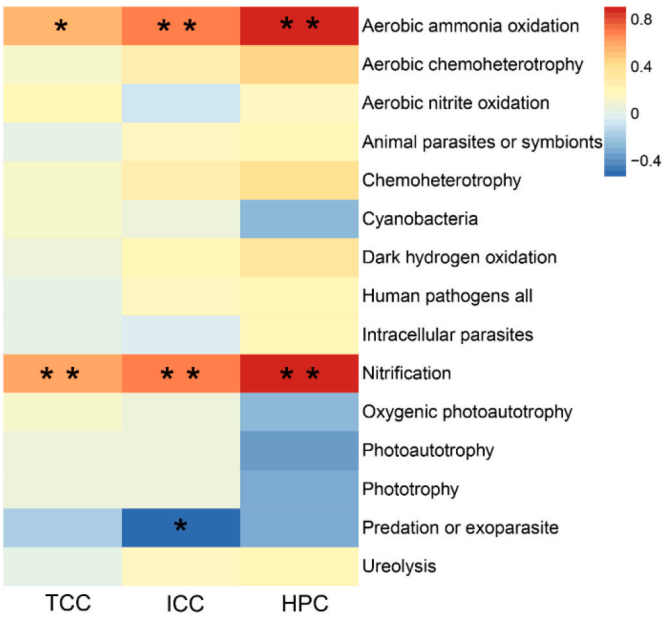

Fig. 4. Spearman correlations among bacterial function annotations and biomass, including TCC, ICC, and HPC. The top 15 functions in abundance based on FAPROTAX are shown in the heat map. **: $p < 0.01$; *: $p < 0.05$.

the abundance of nearly all nitrogen cycle functions slightly decreased after the waterworks, including denitrification, nitrate reduction, nitrogen respiration, and nitrous oxide denitrification (Fig. S8).

Spearman correlations among the biomass and bacterial functional annotations were performed to explore the metabolic process that caused the increased biomass. Functions that are significantly related to biomass include aerobic ammonia oxidation, nitrification, and predation or exoparasite (Fig. 4). In particular, nitrification (R^2=0.575, R^2=0.710, and R^2=0.904) and aerobic ammonia oxidation (R^2=0.543, R^2=0.690, and R^2=0.884) were significant and positively related to all biomass indicators, including TCC, ICC, and HPC.

Spearman correlations between the pipeline lengths and the predicted functions were analyzed (Tab. S7). Pipeline lengths were significantly correlated with nitrification (R^2=0.811, $p < 0.001$) and aerobic ammonia oxidation (R^2=0.801, p=0.001). The nitrogen cycle showed a strong response to pipeline length. Therefore, AOB, nitrite-oxidizing bacteria (NOB), and nitrification products were analyzed. AOB (R^2=0.767, p=0.001) and nitrite (R^2=0.688, p=0.007) were significantly positively correlated with pipeline lengths.

3.4. Potential drivers of sharp biomass increase in SWSS

To explore the potential main drivers of the sharp increase of biomass in the SWSS, we identified the main microbial predictors for HPC, TCC, and ICC in the water samples (which included water in DWTS, DWDS, and SWSS) by RF analysis. The percentage increases of the mean squared error (MSE) of the variables were used to estimate the importance of the predictors. Higher MSE% values imply more important predictors. Nitrifiers and nitrification were regarded as predictors because of the high correlation between nitrification and biomass. The dominant microbes of bacteria, fungi, and algae (Fig. 3) in the SWSS can also be treated as predictors.

Nitrification, aerobic ammonia oxidation, AOB, and Nitrosomonadales were found to be important variables ($p < 0.05$) for predicting biomass (Fig. 5). Burkholderiales and Sphingomonadales could be predictors for HPC and ICC, respectively. However, aerobic nitrite oxidation and NOB cannot be predictors of biomass. In addition, none of the fungi or algae were found to be biomass predictors via RF analysis. Mantel analysis was used to test the effect of nitrifiers on community structures. The results showed that AOB had significant effects on the bacterial (R^2=0.776, $p < 0.001$); fungal (R^2=0.668, $p < 0.001$); and algal (R^2=0.663, $p < 0.001$) community structures.

3.5. Cluster hubs of the microbial correlation network

A biological correlation network was constructed based on the Spearman's rank correlation coefficient matrix of the relative abundances of 491 genera, including bacteria, fungi, and algae, from all water samples, including water in the DWTS, DWDS, and SWSS. The nodes and edges were filtered according to the network degree, which was between 10 and 100 (Fig. S9). The topological properties of the stochastic network with the same scale as the water network were compared with the real water network (Tab. S8). As a result, the σ index (σ>1) indicated that the water microbial network formed a small-world topology. Interconnectivity among bacteria, fungi, and algae was present in the water supply system. Bacteria (84.06%) comprised the most abundant domain. Fungi and algae were less abundant at 12.95% and 2.99%, respectively (Fig. S9a). The core genus that was present in all samples had an abundance of 23.71% (Fig. S9b).

Five modules (clusters 1 to 5) were clustered in the network (Fig. 6a). Clusters 1 and 2, which consist of the vast majority of the core genera

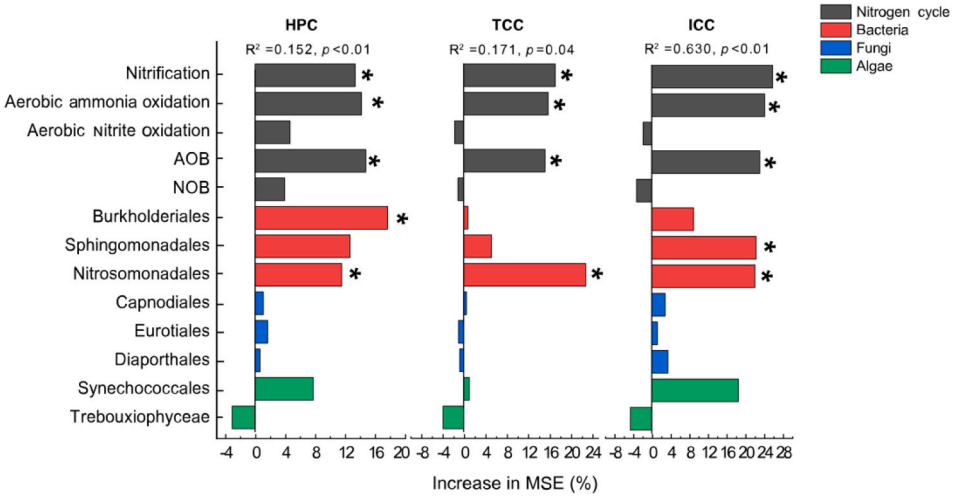

Fig. 5. Potential drivers of biomass in the full-scale drinking water system. The percentage of increase in mean square error random forest indicates the predictor importance (percentage of increase in MSE) of the nitrogen cycle, bacteria, fungi, and algae as drivers of biomass. *: significance drivers.

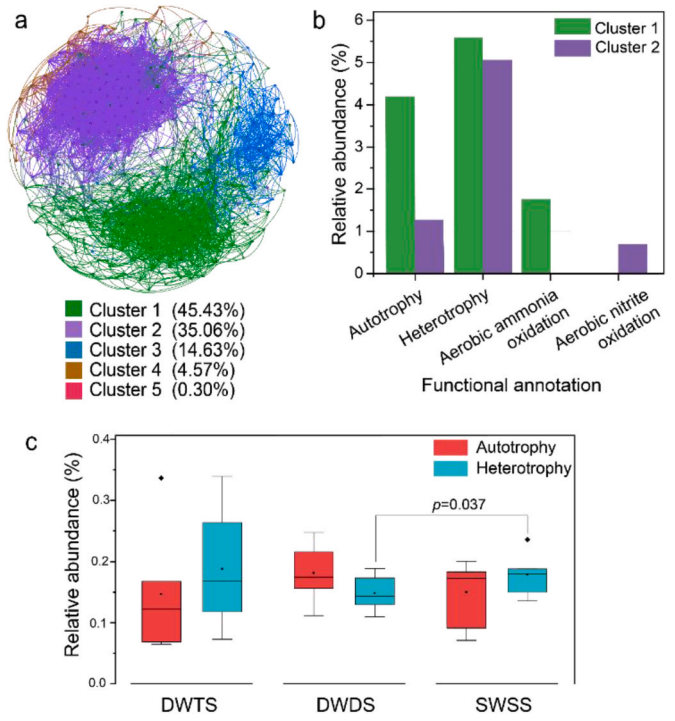

Fig. 6. Whole-community networks of bacteria, fungi, and algae in the full-scale drinking water supply system. Networks were colored according to the cluster module (a). The edge widths are proportional to the Spearman's correlation coefficients between each genus. Functional annotation of network clusters related to assimilation and nitrification in the drinking water system based on FAPROTAX (b). Changes in the relative abundances of autotrophy and heterotrophy among the DWTS, DWDS, and SWSS (c).

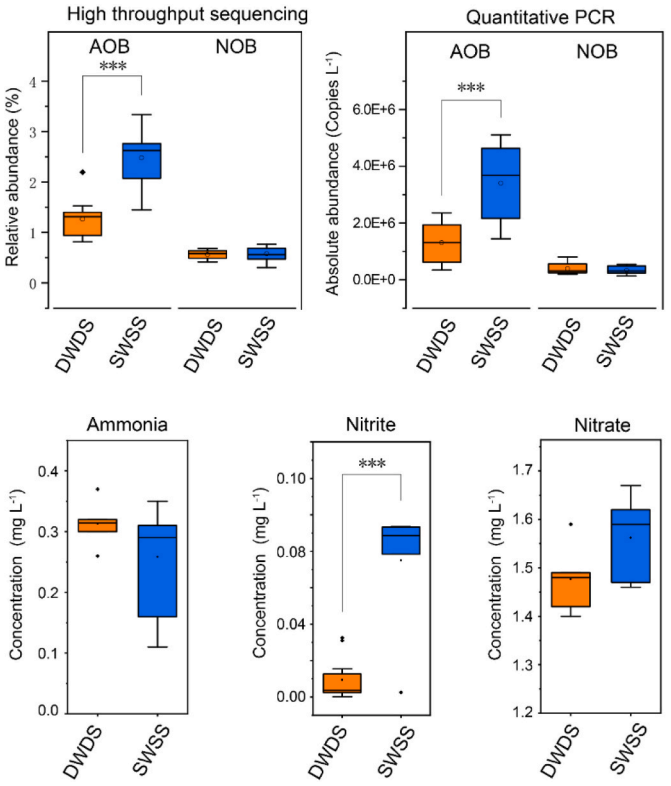

Fig. 7. Comparison of nitrification in the DWDS and SWSS by using Fisher's least significant difference test. Indicators for characterizing nitrification intensity, including the relative and absolute abundances of AOB and NOB, by using 16S high-throughput sequencing and qPCR, respectively, and the concentrations of ammonia nitrogen, nitrite and nitrate nitrogen. ***: $p < 0.001$.

(45.43% and 35.06%, respectively), contributed to the main ecological functions. As nitrifying bacteria, AOB and NOB comprised the core genera in the water supply system. Furthermore, we explored the functional profiles of the ecological modules through FAPROTAX analysis, and nitrogen cycle function annotations were found in cluster 1 and cluster 2. The function of cluster 1 was related to aerobic ammonia oxidation, whereas cluster 2 was related to aerobic nitrite oxidation (Fig. 6b). Therefore, ammonia and nitrite oxidation metabolize separately and were conducted by two different biological clusters. Additionally, the abundances of autotrophy and heterotrophy in cluster 1 were higher than those in cluster 2, indicating that the assimilation of the ammonia oxidation cluster was more vigorous than that of the nitrite oxidation cluster. Furthermore, the assimilation function among different systems was compared (Fig. 6c). The relative abundances of heterotrophy significantly increased from the DWDS to SWSS (Fisher's test, $p < 0.05$), whereas there were no significant differences in the relative abundances of autotrophy between the DWDS and SWSS. Therefore, the increased microbe levels were mainly heterotrophic in the SWSS.

Both the 16S high-throughput sequencing and qPCR results showed that the abundance of AOB in the SWSS was higher than that in the DWDS (Fig. 7). Nitrite concentrations, as the product of ammonia oxidation, were also higher in the SWSS (Fig. 7). Additionally, there were no significant differences in ammonia and nitrate between the DWDS and SWSS.

3.6. Co-occurrence patterns among nitrifiers and microorganisms

To characterize the nitrification pathway in the drinking water supply system, we analyzed the metabolic pathway of nitrogen metabolism (KEGG ko00910) and variations in enzymes. There were no significant differences in the relative abundances of ammonia

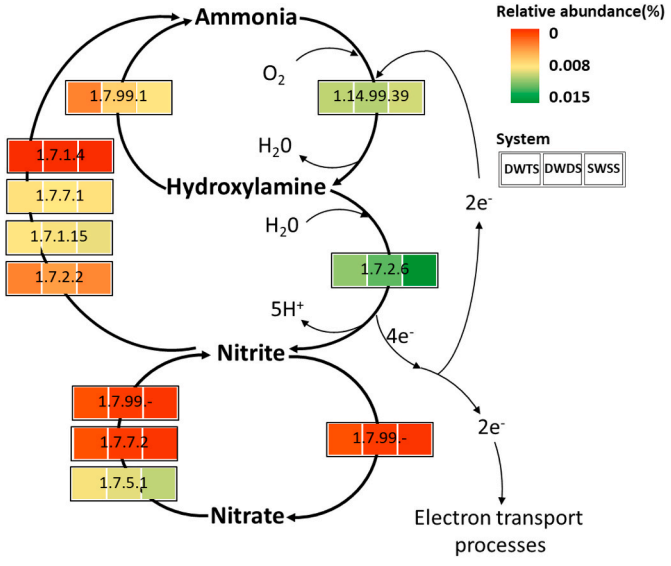

Fig. 8. The differential relative abundances of enzymes involved in the nitrification and denitrification processes among the three subsystems using KEGG-based shotgun metagenomic analyses. Each numbered rectangle represents the participating enzymes.

monooxygenase (EC 1.14.99.39), which can catalyze the oxidation of ammonia to hydroxylamine in all water systems (Fig. 8). Hydroxylamine dehydrogenase (EC 1.7. 2.6), which can catalyze the oxidation of hydroxylamine to nitrite, was enriched in the DWDS and peaked in the SWSS. The enzymes involved in nitrite oxidation (EC 1.7.99.-) and

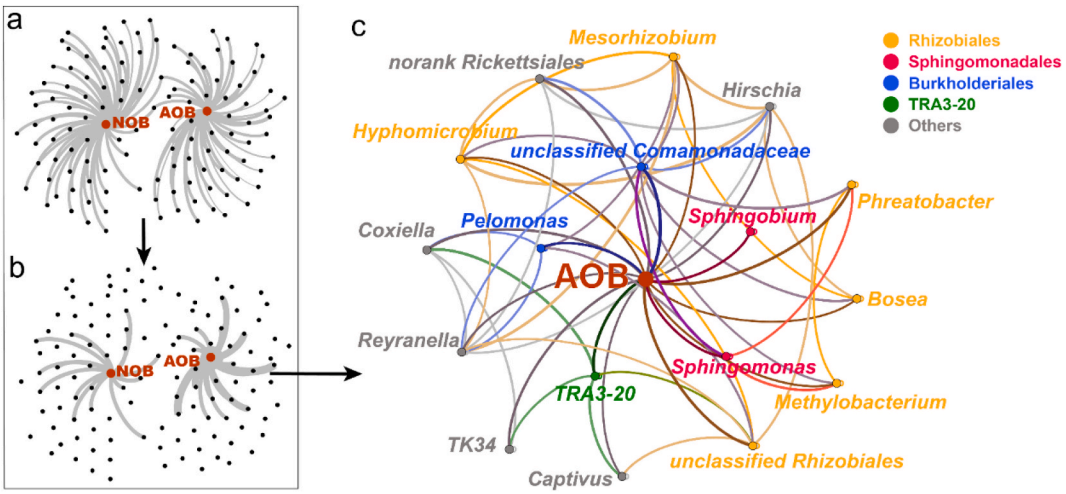

Fig. 9. Co-occurrence network of the biological correlation relationships among nitrifiers and microbes. All edges were visible (a), and 30% of edges were visible based on weight (b). The high-weight network of correlation relationships among AOB and microbes is colored according to order (c).

denitrification were characterized by low abundances in all subsystems. As a result, nitrification in the drinking water supply system was incomplete due to an absence of the related enzyme. In addition, ammonia oxidation in the SWSS was more vigorous than that in the DWDS.

The co-occurrence network of biological correlations among nitrifiers and microorganisms of all water samples was explored. The microorganisms that were associated with nitrifying bacteria included 93.44% bacteria, 3.28% fungi, and 3.28% algae (Fig. 9a, S10). The top 30% edges were selected based on the edge weights (Fig. 9b). Because of incomplete nitrification, the high weight network of correlations between AOB and microbes was analyzed. Most microbes that were highly associated with AOB were heterotrophic bacteria (Fig. 9c). The microorganisms with high abundances in the SWSS, as determined by Wilcoxon rank-sum tests (Fig. 3), such as Sphingomonadales and Burkholderiales, were positively correlated with AOB. Additionally, the iron-oxidizing bacteria, *TRA3-20,* and biofilm bacteria, which included some of the Rhizobiales and Sphingomonadales, showed positive correlations with AOB.

4. Discussion

4.1. Metabolism may affect the sharp increase in biomass in the SWSS

In this study, we focused on the metabolic mechanism of largely microbial regrowth in the SWSS. The biomass amounts remained at low levels in the DWDS, but the biomass properties between the DWDS and SWSS was found to be significantly different. We noted that some species of Burkholderiales, the most abundant bacteria in the SWSS, could not be cultivated on R2A medium (Willems, 2014). Additionally, *Coxiella*, *Bosea,* and *Reyranell*a are difficult to grow on conventional axenic cultivation media (Kazar, 2005; Thomas et al., 2007; Pagnier et al., 2011). ICC increased more than HPC from the DWDS to the SWSS, which may be due to the unavailability of many uncultivated bacteria in drinking water. Thus, measuring ICCs for bacterial characterization is particularly important when evaluating biomass in drinking water supply systems. Furthermore, there was a significant increase in the ratio of ICC to TCC in the SWSS compared with the DWDS, which may be due to the presence of membrane-damaged bacteria in a high chlorine environment and self-repair after chlorine decay. A dramatic increase in ICCs was also found in chlorinated water systems (Nescerecka et al., 2018).

In this study, the biomass amounts in the effluent water increased slightly after a long period of stagnation (8 days) in a full-scale experiment, and the stagnation time was much longer than that of the actual environmental water samples (20 h) in the SWSS. In particular, the beta diversity results revealed that the bacterial, fungal, and algal communities for the DWDS and SWSS were similar. Hence, no obvious exogenous microbial invasion occurred in the SWSS. The sharp increase in biomass in the SWSS was not only due to chloramine decay, but attention should also be paid to microbial metabolism.

4.2. Ammonia oxidation was the dominant driver of microbial regrowth in the SWSS

Previous studies have shown that increases in nitrite and nitrate nitrogen were associated with high HPCs (Wilczak et al., 1996). In our study, nitrification was ubiquitous throughout the system and was one of the metabolisms that was most significantly related to biomass. Additionally, ammonia oxidation showed a strong response to pipeline length. RF analysis suggested that nitrification and aerobic ammonia oxidation were important variables for predicting biomass variations.

Network analysis indicated that interactions were widely found among bacteria, fungi, and algae. It was found that ammonia and nitrite oxidation metabolize separately and were conducted by two different biological clusters, while the metabolism of the ammonia oxidation cluster was more vigorous. Similar to a previous study (Cai et al., 2018), AOB and NOB are competitive in oligotrophic environments, and their activities depend on the synergistic relationships among the two guilds.

The use of chloramines for disinfection can lead to a release of free ammonia as the substrate for AOB growth (Chen et al., 2006; Tatari et al., 2017). In our water system, dissolved oxygen (1.45–3.13 mg L^{-1}), pH (7.16–7.82), temperature (20.4–25.4 °C), and alkalinity (62.55–106.34 mg L^{-1} $CaCO_3$) were sufficient to support complete ammonia oxidation according to previous research (Zhang et al., 2009). The carbon-nitrogen ratios were between 10.13 and 98.35, which were greater than 8.5; therefore, nitrite oxidation was the rate-limiting step for nitrification. The abundances of ammonia oxidation bacteria, concentration of nitrogen species, and related enzymes showed that ammonia oxidation in the SWSS was more vigorous than that in the DWDS. As the enzymes for ammonia oxidation, the relative abundances of hydroxylamine dehydrogenase instead of ammonia monooxygenase were higher in the SWSS. Four electrons are released after hydroxylamine dehydrogenation. Half of these electrons support ammonia oxidation, and the other two electrons pass through the electron transport chain to provide energy for all metabolic processes by generating a proton gradient for ATP generation and by providing a reductant for other cellular processes (Poughon et al., 2001).

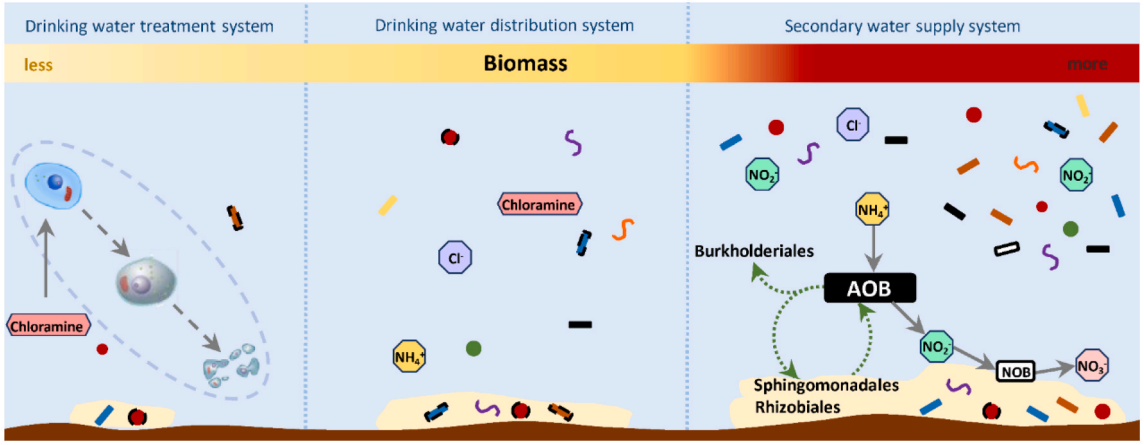

Fig. 10. The synergistic relationships between nitrification and microbial regrowth in community tap water in the full-scale chloraminated water supply system.

4.3. Interaction of AOB and heterotrophic bacteria promotes microbial regrowth in the SWSS

There were strong interactions among nitrifiers and other microorganisms. The contribution of bacteria to AOB interactions was approximately 93.44%, and the contribution of both fungi and algae was 3.28%. Nitrification was conducted by both AOB and ammonia-oxidizing archaea, and bacteria were the principal agents, based on previous studies (Wang et al., 2017; Crenshaw et al., 2008). First, the high correlation between AOB and the iron-oxidizing bacteria, *TRA3-20,* indicated that ammonia oxidation might promote pipeline corrosion and ultimately lead to bacterial growth (Nicomrat et al., 2008). Second, AOB can support heterotroph growth by producing soluble matter and organic compounds in the system without organic carbon (Regan et al., 2003). Thus, heterotroph, including Sphingomonadales and Burkholderiales, which had high abundances in the SWSS, increased with the accumulation of AOB. Third, some heterotrophs can produce extracellular polymers, such as Sphingomonadales, *Hyphomicrobium*, *Mesorhizobium*, *Phreatobacter,* and *Bosea*, that can improve the aggregation of AOB into biofilms. As a result, AOB might be protected by biofilms (Thomas et al., 2007; Tóth et al., 2014). Overall, there were strong relationships among AOB and other bacteria in the water environment. Incomplete nitrification products were involved in the metabolism of heterotrophic bacteria and promoted the growth of heterotrophic bacteria in the SWSS. The protective effect of biofilms on AOB promoted the growth of AOB and incomplete nitrification. The synergistic interaction between AOB and heterotrophic bacteria eventually led to the biomass increase of biomass in tap water (Fig. 10).

In some extreme environments, such as semiarid soil ecosystems, fungal rather than bacterial pathways dominate the transformation of nitrogen (McLain and Martens, 2005, 2006). Furthermore, nitrifiers in microalgal-bacterial systems do not inhibit algal activity, and algae can be used to support nitrification in a photobioreactor (Karya et al., 2013; Rada-Ariza et al., 2017). Therefore, mutual promotion with nitrifying bacteria was not limited to heterotrophic bacteria. Fungi and algae may also play a crucial role in nitrification.

5. Conclusion

In this research, we explored the causes of microbial regrowth in community tap water. Disinfectant decay and stagnation are important reasons for tap water quality deterioration. However, the amount of biomass in the effluent water increased only slightly after a long period of stagnation in a pilot-scale facility experiment, which was different from the rapid increase in microorganisms that was observed for real community tap water. Incomplete nitrification metabolism might play a crucial role in the sharp biomass increase in the SWSS.

Statistical analysis revealed that ammonia oxidation was the dominant driver of the biomass increase in the SWSS. The abundance of ammonia oxidation bacteria, concentration of nitrogen species, and related enzymes indicated that ammonia oxidation in the SWSS was more vigorous than that in the DWDS. Ammonia and nitrite oxidation metabolism were conducted by two different biological clusters. In this drinking water supply system, the metabolism of the ammonia oxidation cluster was more vigorous, and AOB were the dominant nitrifying bacteria. Incomplete nitrification products were involved in the metabolism of heterotrophic bacteria and promoted the growth of heterotrophic bacteria in the SWSS.

This research provides new insights into the relationships between nitrification and microbial regrowth. More attention should be paid to incomplete nitrification, and more work is needed to identify effective measures to control nitrification to reduce microbial regrowth in chloraminated drinking water supply systems to obtain good and safe drinking water.

Declaration of competing interest

The authors declare that they have no known competing financial interests or personal relationships that could have appeared to influence the work reported in this paper.

Acknowledgments

This research was supported by the key Special Program of the Science and Technology for the Pollution Control and Treatment of Water Bodies (2017ZX07207-004, 2017ZX07207-005), the National Natural Science Foundation of China (51878406).

Appendix A. Supplementary data

Supplementary data to this article can be found online at https://doi.org/10.1016/j.envres.2021.111252.

References

Adams, R.I., Miletto, M., Taylor, J.W., Bruns, T.D., 2013. Dispersal in microbes: fungi in indoor air are dominated by outdoor air and show dispersal limitation at short distances. ISME J. 7, 1262–1273. https://doi.org/10.1038/ismej.2013.28.

Albers, C.N., Ellegaard-Jensen, L., Hansen, L.H., Sørensen, S.R., 2018. Bioaugmentation of rapid sand filters by microbiome priming with a nitrifying consortium will optimize production of drinking water from groundwater. Water Res. 129, 1–10. https://doi.org/10.1016/j.watres.2017.11.009.

Bastian, M., H S, J.M., 2009. Gephi: an open source software for exploring and manipulating networks. Icwsm 8, 361–362. https://doi.org/10.13140/2.1.1341.1520.

Berry, D., Xi, C., Raskin, L., 2006. Microbial ecology of drinking water distribution systems. Curr. Opin. Biotechnol. 17, 297–302. https://doi.org/10.1016/j.copbio.2006.05.007.
Bolger, A.M., Lohse, M., Usadel, B., 2014. Trimmomatic: a flexible trimmer for Illumina sequence data. Bioinformatics 30, 2114–2120. https://doi.org/10.1093/bioinformatics/btu170.
Cai, M., Ng, S., Lim, C.K., Lu, H., Jia, Y., et al., 2018. Physiological and metagenomic characterizations of the synergistic relationships between ammonia- and Nitrite-Oxidizing bacteria in freshwater nitrification. Front. Microbiol. 9 https://doi.org/10.3389/fmicb.2018.00280.
Chen, S., Ling, J., Blancheton, J., 2006. Nitrification kinetics of biofilm as affected by water quality factors. Aquacult. Eng. 34, 179–197. https://doi.org/10.1016/j.aquaeng.2005.09.004.
Chen, S., Zhou, Y., Chen, Y., Gu, J., 2018. Fastp: an ultra-fast all-in-one FASTQ preprocessor. Bioinformatics 34, i884–i890. https://doi.org/10.1093/bioinformatics/bty560.
Chen, Y., Su, J., Zhang, J., Li, P., Chen, H., et al., 2019. High-throughput profiling of antibiotic resistance gene dynamic in a drinking water river-reservoir system. Water Res. 149, 179–189. https://doi.org/10.1016/j.watres.2018.11.007.
Crenshaw, C.L., Lauber, C., Sinsabaugh, R.L., Stavely, L.K., 2008. Fungal control of nitrous oxide production in semiarid grassland. Biogeochemistry 87, 17–27. https://doi.org/10.1007/s10533-007-9165-4.
Cruz, M.C., Woo, Y., Flemming, H., Wuertz, S., 2020. Nitrifying niche differentiation in biofilms from full-scale chloraminated drinking water distribution system. Water Res. 176, 115738. https://doi.org/10.1016/j.watres.2020.115738.
Dixon, P., 2003. VEGAN, a package of R functions for community ecology. J. Veg. Sci. 14, 927–930. https://doi.org/10.1111/j.1654-1103.2003.tb02228.x.
Douterelo, I., Sharpe, R.L., Boxall, J.B., 2013. Influence of hydraulic regimes on bacterial community structure and composition in an experimental drinking water distribution system. Water Res. 47, 503–516. https://doi.org/10.1016/j.watres.2012.09.053.
Edgar, R.C., 2013. UPARSE: highly accurate OTU sequences from microbial amplicon reads. Nat. Methods 10, 996–998. https://doi.org/10.1038/nmeth.2604.
Edgar, R.C., Haas, B.J., Clemente, J.C., Quince, C., Knight, R., 2011. UCHIME improves sensitivity and speed of chimera detection. Bioinformatics 27, 2194–2200. https://doi.org/10.1093/bioinformatics/btr381.
Graham, D.W., Knapp, C.W., Van Vleck, E.S., Bloor, K., Lane, T.B., et al., 2007. Experimental demonstration of chaotic instability in biological nitrification. ISME J. 1, 385–393. https://doi.org/10.1038/ismej.2007.45.
Gülay, A., Musovic, S., Albrechtsen, H., Al-Soud, W.A., Sørensen, S.J., et al., 2016. Ecological patterns, diversity and core taxa of microbial communities in groundwater-fed rapid gravity filters. ISME J. 10, 2209–2222. https://doi.org/10.1038/ismej.2016.16.
Jiao, S., Chen, W., Wang, J., Du, N., Li, Q., et al., 2018. Soil microbiomes with distinct assemblies through vertical soil profiles drive the cycling of multiple nutrients in reforested ecosystems. Microbiome 6, 146–158. https://doi.org/10.1186/s40168-018-0526-0.
Karya, N.G.A.I., van der Steen, N.P., Lens, P.N.L., 2013. Photo-oxygenation to support nitrification in an algal–bacterial consortium treating artificial wastewater. Bioresour. Technol. 134, 244–250. https://doi.org/10.1016/j.biortech.2013.02.005.
Kazar, J., 2005. Coxiella burnetii infection. Ann. N. Y. Acad. Sci. 105–114.
Lautenschlager, K., Hwang, C., Liu, W., Boon, N., Köster, O., et al., 2013. A microbiology-based multi-parametric approach towards assessing biological stability in drinking water distribution networks. Water Res. 47, 3015–3025. https://doi.org/10.1016/j.watres.2013.03.002.
Lehtinen, J., Nuutila, J., Lilius, E., 2004. Green fluorescent protein-propidium iodide (GFP-PI) based assay for flow cytometric measurement of bacterial viability. Cytometry 60A, 165–172. https://doi.org/10.1002/cyto.a.20026.
Li, H., Li, S., Tang, W., Yang, Y., Zhao, J., et al., 2018. Influence of secondary water supply systems on microbial community structure and opportunistic pathogen gene markers. Water Res. 136, 160–168. https://doi.org/10.1016/j.watres.2018.02.031.
Li, R., Yu, C., Li, Y., Lam, T., Yiu, S., et al., 2009. SOAP2: an improved ultrafast tool for short read alignment. Bioinformatics 25, 1966–1967. https://doi.org/10.1093/bioinformatics/btp336.
Liu, G., Zhang, Y., Knibbe, W., Feng, C., Liu, W., et al., 2017. Potential impacts of changing supply-water quality on drinking water distribution: a review. Water Res. 116, 135–148. https://doi.org/10.1016/j.watres.2017.03.031.
Liu, G., Zhang, Y., van der Mark, E., Magic-Knezev, A., Pinto, A., et al., 2018. Assessing the origin of bacteria in tap water and distribution system in an unchlorinated drinking water system by SourceTracker using microbial community fingerprints. Water Res. 138, 86–96. https://doi.org/10.1016/j.watres.2018.03.043.
Looft, T., Johnson, T.A., Allen, H.K., Bayles, D.O., Alt, D.P., et al., 2012. In-feed antibiotic effects on the swine intestinal microbiome. Proc. Natl. Acad. Sci. U.S.A. 109, 1691–1696. https://doi.org/10.1073/pnas.1120238109.
Louca, S., Parfrey, L.W., Doebeli, M., 2016. Decoupling function and taxonomy in the global ocean microbiome. Science 353, 1272–1277. https://doi.org/10.1126/science.aaf4507.
Matsui, Y., Nakao, S., Sakamoto, A., Taniguchi, T., Pan, L., et al., 2015. Adsorption capacities of activated carbons for geosmin and 2-methylisoborneol vary with activated carbon particle size: effects of adsorbent and adsorbate characteristics. Water Res. 85, 95–102. https://doi.org/10.1016/j.watres.2015.08.017.
McLain, J.E.T., Martens, D.A., 2005. Nitrous oxide flux from soil amino acid mineralization. Soil Biol. Biochem. 37, 289–299. https://doi.org/10.1016/j.soilbio.2004.03.013.
McLain, J.E.T., Martens, D.A., 2006. N2O production by heterotrophic N transformations in a semiarid soil. Appl. Soil Ecol. 32, 253–263. https://doi.org/10.1016/j.apsoil.2005.06.005.
Mori, H., Maruyama, F., Kato, H., Toyoda, A., Dozono, A., et al., 2014. Design and experimental application of a novel Non-Degenerate universal primer set that amplifies prokaryotic 16S rRNA genes with a low possibility to amplify eukaryotic rRNA genes. DNA Res. 21, 217–227. https://doi.org/10.1093/dnares/dst052.
Nescerecka, A., Juhna, T., Hammes, F., 2018. Identifying the underlying causes of biological instability in a full-scale drinking water supply system. Water Res. 135, 11–21. https://doi.org/10.1016/j.watres.2018.02.006.
Nguyen, N.H., Song, Z., Bates, S.T., Branco, S., Tedersoo, L., et al., 2016. FUNGuild: an open annotation tool for parsing fungal community datasets by ecological guild. Fungal Ecology 20, 241–248. https://doi.org/10.1016/j.funeco.2015.06.006.
Nicomrat, D., Dick, W.A., Dopson, M., Tuovinen, O.H., 2008. Bacterial phylogenetic diversity in a constructed wetland system treating acid coal mine drainage. Soil Biol. Biochem. 40, 312–321. https://doi.org/10.1016/j.soilbio.2007.08.009.
Nilsson, R.H., Larsson, K., Taylor, A.F.S., Bengtsson-Palme, J., Jeppesen, T.S., et al., 2019. The UNITE database for molecular identification of fungi: handling dark taxa and parallel taxonomic classifications. Nucleic Acids Res. 47, D259–D264. https://doi.org/10.1093/nar/gky1022.
Pagnier, I., Raoult, D., La Scola, B., 2011. Isolation and characterization of Reyranella massiliensis gen. Nov., Sp. Nov. From freshwater samples by using an amoeba co-culture procedure. Int. J. Syst. Evol. Microbiol. 61, 2151. https://doi.org/10.1099/ijs.0.025775-0.
Pfendler, S., Karimi, B., Maron, P., Ciadamidaro, L., Valot, B., et al., 2018. Biofilm biodiversity in French and Swiss show caves using the metabarcoding approach: first data. Sci. Total Environ. 615, 1207–1217. https://doi.org/10.1016/j.scitotenv.2017.10.054.
Poughon, L., Dussap, C., Gros, J., 2001. Energy model and metabolic flux analysis for autotrophic nitrifiers. Biotechnol. Bioeng. 72, 416–433. https://doi.org/10.1002/1097-0290(20000220)72:4<416::AID-BIT1004>3.0.CO, 2-D.
Prest, E.I., Hammes, F., van Loosdrecht, M.C.M., Vrouwenvelder, J.S., 2016. Biological stability of drinking water: controlling factors, methods, and challenges. Front. Microbiol. 7, 45. https://doi.org/10.3389/fmicb.2016.00045.
Quast, C., Pruesse, E., Yilmaz, P., Gerken, J., Schweer, T., et al., 2012. The SILVA ribosomal RNA gene database project: improved data processing and web-based tools. Nucleic Acids Res. 41, D590–D596. https://doi.org/10.1093/nar/gks1219.
Rada-Ariza, A.M., Lopez-Vazquez, C.M., van der Steen, N.P., Lens, P.N.L., 2017. Nitrification by microalgal-bacterial consortia for ammonium removal in flat panel sequencing batch photo-bioreactors. Bioresour. Technol. 245, 81–89. https://doi.org/10.1016/j.biortech.2017.08.019.
Regan, J.M., Harrington, G.W., Baribeau, H., Leon, R.D., Noguera, D.R., 2003. Diversity of nitrifying bacteria in full-scale chloraminated distribution systems. Water Res. 37, 197–205. https://doi.org/10.1016/S0043-1354(02)00237-3.
Schloss, P.D., Westcott, S.L., Ryabin, T., Hall, J.R., Hartmann, M., et al., 2009. Introducing mothur: open-source, platform-independent, community-supported software for describing and comparing microbial communities. Appl. Environ. Microbiol. 75, 7537–7541. https://doi.org/10.1128/AEM.01541-09.
Segata, N., Izard, J., Waldron, L., Gevers, D., Miropolsky, L., et al., 2011. Metagenomic biomarker discovery and explanation. Genome Biol. 12, R60. https://doi.org/10.1186/gb-2011-12-6-r60.
Sherwood, A.R., Presting, G.G., 2007. Universal primers amplify a 23S rDNA plastid marker in eukaryotic algae and cyanobacteria. J. Phycol. 43, 605–608. https://doi.org/10.1111/j.1529-8817.2007.00341.x.
Sigstam, T., Gannon, G., Cascella, M., Pecson, B.M., Wigginton, K.R., et al., 2013. Subtle differences in virus composition affect disinfection kinetics and mechanisms. Appl. Environ. Microbiol. 79, 3455–3467. https://doi.org/10.1128/AEM.00663-13.
Tatari, K., Musovic, S., Gülay, A., Dechesne, A., Albrechtsen, H., et al., 2017. Density and distribution of nitrifying guilds in rapid sand filters for drinking water production: dominance of Nitrospira spp. Water Res. 127, 239–248. https://doi.org/10.1016/j.watres.2017.10.023.
Thomas, V., Casson, N., Greub, G., 2007. New Afipia and Bosea strains isolated from various water sources by amoebal co-culture. Syst. Appl. Microbiol. 30, 572–579. https://doi.org/10.1016/j.syapm.2007.06.004.
Tóth, E.M., Vengring, A., Homonnay, Z.G., Kéki, Z., Spröer, C., et al., 2014. Phreatobacter oligotrophus gen. Nov., Sp. Nov., an alphaproteobacterium isolated from ultrapure water of the water purification system of a power plant. Int. J. Syst. Evol. Microbiol. 64, 839. https://doi.org/10.1099/ijs.0.053843-0.
Wagner, F.B., Nielsen, P.B., Boe-Hansen, R., Albrechtsen, H., 2018. Remediation of incomplete nitrification and capacity increase of biofilters at different drinking water treatment plants through copper dosing. Water Res. 132, 42–51. https://doi.org/10.1016/j.watres.2017.12.061.
Wang, Q., Garrity, G.M., Tiedje, J.M., Cole, J.R., 2007. Naive bayesian classifier for rapid assignment of rRNA sequences into the new bacterial taxonomy. Appl. Environ. Microbiol. 73, 5261–5267. https://doi.org/10.1128/AEM.00062-07.
Wang, Y., Ma, L., Mao, Y., Jiang, X., Xia, Y., et al., 2017. Comammox in drinking water systems. Water Res. 116, 332–341. https://doi.org/10.1016/j.watres.2017.03.042.
Wilczak, A., Jacangelo, J.G., Marcinko, J.P., Odell, L.H., Kirmeyer, G.J., et al., 1996. Occurrence of nitrification in chloraminated distribution systems. Journal (American Water Works Association) 88, 74–85. https://doi.org/10.1002/j.1551-8833.1996.tb06586.x.
Willems, A., 2014. The family Comamonadaceae. In: Rosenberg, E., DeLong, E.F., Lory, S., Stackebrandt, E., Thompson, F. (Eds.), The Prokaryotes. Springer, Berlin, Heidelberg.
Xie, X., Liu, N., Yang, B., Yu, C., Zhang, Q., et al., 2016. Comparison of microbial community in hydrolysis acidification reactor depending on different structure dyes

by Illumina MiSeq sequencing. Int. Biodeterior. Biodegrad. 111, 14–21. https://doi.org/10.1016/j.ibiod.2016.04.004.

Xu, H., Lin, C., Chen, W., Shen, Z., Liu, Z., et al., 2018. Effects of pipe material on nitrogen transformation, microbial communities and functional genes in raw water transportation. Water Res. 143, 188–197. https://doi.org/10.1016/j.watres.2018.06.040.

Zamyadi, A., Henderson, R., Stuetz, R., Hofmann, R., Ho, L., et al., 2015. Fate of geosmin and 2-methylisoborneol in full-scale water treatment plants. Water Res. 83, 171–183. https://doi.org/10.1016/j.watres.2015.06.038.

Zhang, K., Gao, Y., Du, M., Liu, S., Dong, C., et al., 2019. Vgas: a viral genome annotation system. Front. Microbiol. 10, 184. https://doi.org/10.3389/fmicb.2019.00184.

Zhang T, Q.X.L.F., 2007. Use of P-17 and NOX specific primer sets for assimilable organic carbon (AOC) measurements. Water Sci. Technol. Water Supply 7, 157–163. https://doi.org/10.2166/ws.2007.050.

Zhang, Y., Love, N., Edwards, M., 2009. Nitrification in drinking water systems. Crit. Rev. Environ. Sci. Technol. 39, 153–208. https://doi.org/10.1080/10643380701631739.

Zheng, J., Zhou, Z., Wei, Y., Chen, T., Feng, W., et al., 2018. High-throughput profiling of seasonal variations of antibiotic resistance gene transport in a peri-urban river. Environ. Int. 114, 87–94. https://doi.org/10.1016/j.envint.2018.02.039.